Available online at www.sciencedirect.com
ScienceDirect
Bioorganic & Medicinal Chemistry Letters 18 (2008) 3446–3455
Bioorganic & Medicinal Chemistry Letters

Novel HCV NS5B polymerase inhibitors derived from 4-(1′,1′-dioxo-1′,4′-dihydro-1′λ^6-benzo[1′,2′,4′]thiadiazin-3′-yl)-5-hydroxy-2*H*-pyridazin-3-ones. Part 3: Further optimization of the 2-, 6-, and 7′-substituents and initial pharmacokinetic assessments

Lian-Sheng Li, Yuefen Zhou,* Douglas E. Murphy, Nebojsa Stankovic, Jingjing Zhao, Peter S. Dragovich, Thomas Bertolini, Zhongxiang Sun, Benjamin Ayida, Chinh V. Tran, Frank Ruebsam, Stephen E. Webber, Amit M. Shah, Mei Tsan, Richard E. Showalter, Rupal Patel, Laurie A. LeBrun, Darian M. Bartkowski, Thomas G. Nolan, Daniel A. Norris, Ruhi Kamran, Jennifer Brooks, Maria V. Sergeeva, Leo Kirkovsky, Qiang Zhao and Charles R. Kissinger

Anadys Pharmaceuticals, Inc., 3115 Merryfield Row, San Diego, CA 92121, USA

Received 5 February 2008; revised 27 February 2008; accepted 28 February 2008
Available online 5 March 2008

Abstract—5-Hydroxy-3(2*H*)-pyridazinone derivatives were investigated as inhibitors of genotype 1 HCV NS5B polymerase. Lead optimization led to the discovery of compound **3a**, which displayed potent inhibitory activities in biochemical and replicon assays [IC_{50} (1b) < 10 nM; IC_{50} (1a) = 22 nM; EC_{50} (1b) = 5 nM], good stability toward human liver microsomes (HLM $t_{1/2}$ > 60 min), and high ratios of liver to plasma concentrations 12 h after a single oral administration to rats.

Hepatitis C virus (HCV) is a major cause of chronic liver disease, including cirrhosis and liver cancer. Globally, an estimated 170 million individuals, 3% of the world's population, are chronically infected with HCV and an estimated 4 million people are newly infected each year.[1] Currently, there is no vaccine available to prevent hepatitis C nor a direct antiviral agent available for the treatment of chronic hepatitis C.

The current standard of care is a combination of pegylated interferon (IFN) with ribavirin.[2] Inadequate response rates, in particular for patients infected with genotype 1 HCV, along with significant side-effects of current HCV therapy result in an urgent medical need for improved treatments.[3]

As part of our efforts to develop small molecule, non-nucleoside inhibitors of the HCV NS5B enzyme, a virally encoded RNA-dependent RNA polymerase (RdRp) essential for HCV replication,[4] we previously described the discovery and structure-based optimization of a series of 5-hydroxy-3(2*H*)-pyridazinone derivatives which bind to the NS5B 'palm' site (**1**, Fig. 1).[5,6] In the course of this work, we identified compound **2**

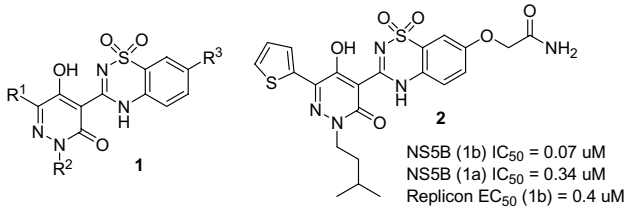

Figure 1. HCV NS5B polymerase inhibitors.

Keywords: Pyridazinones; 5-Hydroxy-3(2*H*)-pyridazinone derivatives; Hepatitis C virus (HCV); RNA-dependent RNA polymerase (RdRp); Small molecule; Non-nucleoside NS5B inhibitors; DMPK profiling; Ratio of liver to plasma concentration.
* Corresponding author. Tel.: +1 858 273 2501x221; fax: +1 858 273 2697; e-mail: yuefen.zhou@gmail.com

0960-894X/$ - see front matter © 2008 Published by Elsevier Ltd.
doi:10.1016/j.bmcl.2008.02.072

(Fig. 1) bearing an acetamide R^3 moiety as one of the most potent NS5B inhibitors and antiviral agents.

Here, we report the further optimization and preliminary pharmacokinetic profiling of this series of pyridazinone-containing NS5B inhibitors. Since during our previous studies we observed that R^3 substitution had the most significant impact on inhibitor potency,[5] we chose to continue making modifications at this position.

As shown in Table 1, when the $-OCH_2CONH_2$ moiety present in compound **2** was replaced by a $-NHSO_2Me$ fragment, the resulting compound (**3a**) displayed dramatically improved NS5B inhibitory potency and antiviral activity.[10] This significant increase in potency could be explained with the aid of the co-crystal structure of **3a** bound to the NS5B protein.

As is depicted in Figure 2, the $-NHSO_2Me$ R^3 moiety of **3a** formed H-bonds with NS5B residues Asn291 and Asp318. Similar H-bonding interactions were also observed in the **2**–NS5B co-crystal structure between the acetamide moiety of compound **2** and NS5B.[6] Importantly, the $-NHSO_2Me$ R^3 moiety of **3a** formed a third H-bond network with the residue Ser288 via a water molecule that was absent in the **2**–NS5B co-crystal structure. This additional H-bond network, which complements a similar interaction from the $-SO_2-$ moiety in the benzothiadiazine ring of **3a** (Fig. 2), is likely responsible for the potency differences observed between compounds **2** and **3a**.[12]

Although the above co-crystal structure indicated that the methyl substituent of the $-NHSO_2Me$ R^3 moiety present in **3a** was oriented away from the NS5B surface, increasing the size of this fragment was generally detrimental to anti-NS5B and antiviral properties (Table 1, compounds **3b**–**3g**). However, this methyl group could be replaced with an $-NH_2$ moiety without sacrificing antiviral potencies (**3h**). Other, often drastic, losses in NS5B inhibition activity and antiviral properties were noted for compounds in which the NH of the R^3 sulfonamide moiety was alkylated (**3i**–**l**) or removed (compounds **3m**–**q**). Such unfavorable property alterations are likely due to the loss of the H-bond noted in Figure 2 between the R^3 sulfonamide NH and the NS5B Asp318 residue.[13] The results described above confirmed the large impact that R^3 variation had on the anti-NS5B and antiviral properties of this series of inhibitors and identified the $-NHSO_2Me$ and $-NHSO_2NH_2$ fragments as optimal R^3 moieties.

We next explored the systematic variation of the R^1 and R^2 substituents attached to the pyridazinone ring of the inhibitors (**1**). Due to its relative ease of synthesis, we employed the $-NHSO_2Me$ moiety in lieu of the $-NHSO_2NH_2$ fragment as the preferred R^3 substituent.

As shown in Table 2, when the 2-thiophene R^1 group present in **3a** was replaced by other unsubstituted five-membered heterocycles identified during our previous studies,[6] the resulting compounds (**4a**–**c**) retained good NS5B inhibition activity and antiviral properties in cell culture. As we also previously observed,[6] appending substituents to such heterocycles were detrimental to the associated biological potencies (**4d**–**e**) as was the incorporation of a six-membered aromatic ring at this location (**4f**). Introduction of alkyl and alkenyl groups (both cyclic and acyclic) at the R^1 position of the inhibitor design (**4g**–**4s**) generally afforded compounds with significantly poorer anti-NS5B and/or antiviral properties relative to **3a**. The most notable exceptions were compounds **4l** and **4m**, which exhibited replicon potencies that were only about fourfold weaker than that displayed by **3a**. While the exact reasons for these structure–activity relationships are not all known, the results described above confirmed that unsubstituted five-membered heterocycles represent ideal R^1 substituents that confer the most potent anti-NS5B and antiviral properties to this series of NS5B inhibitors.

Table 3 summarizes the results obtained from varying the R^2 substituent of pyridazinones containing optimal 2-thiophene R^1 and $-NHSO_2Me$ R^3 moieties.

As previously observed,[6] a R^2 alkyl fragment in linear 4–5 carbon chain length led to both good anti-NS5B and antiviral activities (**5a**–**f**) comparable to that of **3a**. However, more polar R^2 groups with a methoxy moiety at the terminus led to less potent compounds (**5g** and **5h**) (compared with **5c**). Introducing branching at the C-atom of the R^2 fragment adjacent to the pyridazinone N-2 atom was highly detrimental to both anti-NS5B and antiviral properties (compounds **5i**–**k**). Consistent with what we observed previously,[6] shorter R^2 groups such as *iso*-butyl and 2,2-dimethylpropyl (**5l**–**m**) resulted in significant potency loss in 1b replicon assays as compared with **3a**. In general, the saturated cyclic alkyl methyl/ethyl R^2 groups (**5n**–**t**) led to less potent inhibitors as compared with **3a** with the exception of **5p**. Interestingly, analogs containing a benzyl moiety (with or without substitution) or a 2-pyridyl methylene R^2 group (**5u**–**x**) all displayed poor antiviral potency in the 1b replicon assay. Such inhibition properties could be improved by the introduction of a 3-thiophene methylene R^2 group (**5y**). Collectively, the above results demonstrate that numerous aliphatic moieties tethered to the pyridazinone N-2 atom by a methylene group could serve as effective R^2 substituents for this series of NS5B inhibitors.

In general, the pyridazinone-containing NS5B inhibitors described in this work displayed somewhat weaker inhibition activities when tested against genotype 1a HCV polymerase than that against genotype 1b enzyme (Tables 1–3). The difference in these inhibition levels was within sixfold for most compounds, although larger and smaller variations were noted. All of the smaller deviations were detected during the exploration of the pyridazinone R^1 moieties (Table 2: **4i**, **4m**, **4p**, and **4s**) while the larger differences were mostly observed during variation of the R^2 substituents (Table 3: **5g**, **5l**, **5n**–**o**, **5r**–**s**, and **5u**–**x**). Although the structural basis for these potency differences is not known, these results suggest that the described pyridazinone-containing molecules have good potential to inhibit HCV polymerases derived

Table 1. Optimization of R^3 substituents

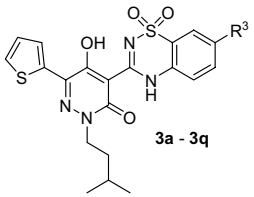

Compound[a]	R^3	IC_{50} (1b)[b] (μM)	IC_{50} (1a)[c] (μM)	EC_{50} (1b)[b] (μM)	CC_{50}[b] (μM)	HLM $t_{1/2}$[b] (min)
3a		<0.01	<0.025	0.005	>33	>60
3b		0.045	0.054	0.098	>33	>60[d]
3c		0.027	0.092	0.043	>1	>60
3d		0.03	0.16	0.25	>1	ND[e]
3e	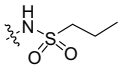	0.038	0.14	0.15	>1	ND
3f	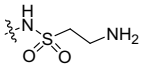	0.019	0.026	0.069	>1	>60
3g	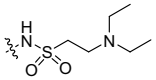	0.17	0.49	0.76	>33	>60
3h[f]		<0.01	0.028	0.007	>1	>60
3i		0.023	0.46	0.13	>33	28
3j		0.25	ND	0.42	>1	11
3k		3.2	ND	ND	ND	ND
3l		0.29	ND	4.8	>33	27
3m[g]		0.15	0.29	0.11	>33	22

Table 1 (*continued*)

Compound[a]	R^3	IC_{50} (1b)[b] (μM)	IC_{50} (1a)[c] (μM)	EC_{50} (1b)[b] (μM)	CC_{50}[b] (μM)	HLM $t_{1/2}$[b] (min)
3n		0.24	ND	1.8	>33	28
3o		0.3	ND	ND	ND	5.6
3p		0.076	1.8	1.5	>33	13[d]
3q		3.2	ND	ND	ND	11

[a] See Ref. 7.
[b] See Refs. 5 (for assay methods and experimental errors) and 8.
[c] See Refs. 6 (for assay method and experimental error) and 9.
[d] Compounds were screened at 5 μM and the other compounds were screened at 1 μM.
[e] ND, not determined.
[f] R^2 = 3,3-dimethylbutyl (R^2 where shown in compound **1**).
[g] Racemic.

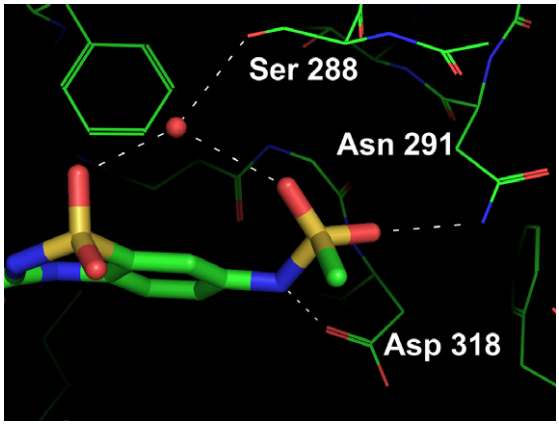

Figure 2. R^3 region of the co-crystal structure of **3a** bound to the NS5B protein.[11] Other protein–ligand interactions were similar to those previously observed between compound **2** and NS5B.[6]

from both 1a and 1b genotypes. However, the data also caution that the selection of truly optimal inhibitor substituents, particularly at the pyridazinone R^2 position, should be made using inhibition values obtained from both genotype 1a and 1b enzymes.

In addition, the antiviral potencies (EC_{50}) of the inhibitors under study measured against genotype 1b HCV replicon were usually weaker (2- to 20-fold) than the corresponding genotype 1b NS5B IC_{50} values (Tables 1–3).[14] However, several exceptions to this general trend were noted (compounds **3m**, **4l–m**, **4p**, **5b–d**, **5g–h**, and **5p**). The differences in the EC_{50}/IC_{50} ratios are likely caused by variations in compound cell permeability and/or protein binding properties. The stability of many pyridazinone-containing inhibitors toward human liver microsomes was also assessed (Tables 1–3), and most compounds tested exhibited moderate to long half-lives ($t_{1/2}$ > 30 min). Notable exceptions included molecules in which the R^3 sulfonamide NH was alkylated or removed (Table 1: **3i–q**) and the inhibitors bearing alkyl or alkenyl R^1 moieties (Table 2: **4g–s**). Importantly, many examples of pyridazinone-containing compounds were identified that combined potent NS5B inhibition properties with good stability toward human liver microsomes.

Encouraged by the above results, we examined the pharmacokinetic properties of two very potent and metabolically stable NS5B inhibitors (**3a** and **5a**) in monkeys after both oral (po) and intravenous (iv) administration of a 5 mg/kg single dose (Table 4).

As expected based on its good in vitro stability toward monkey liver microsomes (MLM), compound **3a** exhibited a low in vivo clearance value after iv administration (Table 4). Somewhat surprisingly, **5a** displayed similar in vivo clearance properties in spite of its reduced MLM stability relative to **3a** (Table 4 and Fig. 3). These results suggested that the in vivo clearance of one or both compounds may not be primarily affected by CYP-mediated biotransformation. Both inhibitors also exhibited low distribution volumes in the iv experiments.

Unfortunately, the bioavailabilities of both compounds (**3a** and **5a**) after oral administration to cynomolgus monkeys were very low. Since the molecules displayed low in vivo clearance values and reasonable solubilities in H_2O at pH 7.4, we believe that their undesirable oral PK properties primarily result from poor gut permeability. Accordingly, both inhibitors displayed very low P_{app} values in Caco-2 permeability assessments (Table 4). These poor permeability properties are consistent with the highly polar nature of both **3a** and **5a** (polar surface

Table 2. Optimization of R^1 substituents

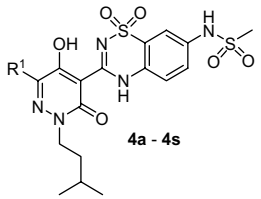

Compound[a]	R^1	IC_{50} (1b)[b] (μM)	IC_{50} (1a)[c] (μM)	EC_{50} (1b)[b] (μM)	CC_{50}[b] (μM)	HLM $t_{1/2}$[b] (min)
3a		<0.01	<0.025	0.005	>33	>60
4a		0.01	0.048	0.008	>33	>60[e]
4b[d]		<0.01	0.047	0.005	>1	31
4c		0.01	0.05	0.007	>1	30
4d		0.047	0.34	0.24	>1	38
4e[d]	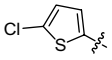	0.14	0.22	1.5	>33	>60
4f		0.031	0.18	0.36	>1	38
4g		0.061	0.19	0.53	>1	7
4h		0.057	0.51	0.41	>1	17
4i		0.071	0.097	0.12	>33	19
4j		0.13	0.4	0.21	>33	25
4k		0.22	ND[f]	0.56	>33	9
4l		0.049	0.21	0.023	>1	56
4m		0.029	<0.025	0.020	>1	33
4n		0.13	0.3	0.81	>33	10

Table 2 (*continued*)

Compound[a]	R^1	IC_{50} (1b)[b] (μM)	IC_{50} (1a)[c] (μM)	EC_{50} (1b)[b] (μM)	CC_{50}[b] (μM)	HLM $t_{1/2}$[b] (min)
4o		0.029	0.093	0.16	>1	6
4p		0.1	0.075	0.1	>1	7.4
4q		0.18	0.6	0.8	>1	6
4r		0.28	ND	1.1	>33	10
4s		0.17	0.26	1.04	>33	31

[a] See Ref. 7.
[b] See Refs. 5 (for assay methods and experimental errors) and 8.
[c] See Refs. 6 (for assay method and experimental error) and 9.
[d] R^2 = cyclopropyl ethyl group (R^2 where shown in compound **1**).
[e] Compound was screened at 5 μM and the other compounds were screened at 1 μM.
[f] ND, not determined.

Table 3. Optimization of R^2 substituents

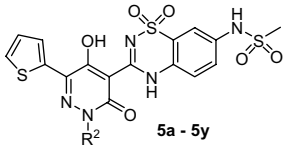

5a - 5y

Compound[a]	R^2	IC_{50} (1b)[b] (μM)	IC_{50} (1a)[c] (μM)	EC_{50} (1b)[b] (μM)	CC_{50}[b] (μM)	HLM $t_{1/2}$[b] (min)
3a	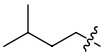	<0.01	<0.025	0.005	>33	>60
5a	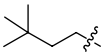	0.01	0.059	0.016	>1	>60
5b	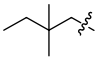	0.024	0.054	0.008	>1	>60
5c	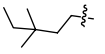	0.019	0.076	0.009	>1	>60
5d[d]	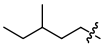	0.011	0.072	0.005	>1	>60
5e	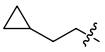	<0.01	0.026	0.004	>33	>60
5f	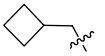	<0.01	<0.025	0.019	>1	>60
5g	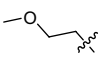	0.027	2.5	0.06	>1	>60[e]
5h	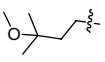	0.027	0.11	0.030	>33	>60

(*continued on next page*)

Table 3 (*continued*)

Compound[a]	R^2	IC_{50} (1b)[b] (μM)	IC_{50} (1a)[c] (μM)	EC_{50} (1b)[b] (μM)	CC_{50}[b] (μM)	HLM $t_{1/2}$[b] (min)
5i[d]	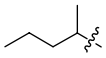	0.59	ND[f]	15	>33	>60
5j[d]	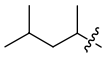	1	ND	16	>33	ND
5k[d]		0.45	ND	11	>33	>60
5l		<0.01	0.3	0.041	>1	>60
5m		0.014	0.077	0.016	>1	>60
5n	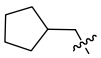	0.01	1.2	0.015	>1	>60
5o		<0.01	0.38	0.034	>1	>60
5p		0.013	0.07	0.007	>1	>60
5q		0.023	0.1	0.032	>1	60
5r	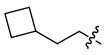	<0.01	0.2	0.08	>1	>60
5s	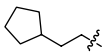	0.018	0.21	0.040	>1	>60
5t	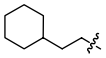	0.19	0.69	3.3	>17	>60
5u	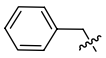	0.011	0.45	0.19	>1	>60
5v	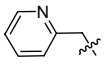	0.033	0.48	0.75	>1	>60
5w	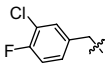	0.012	0.15	0.26	>1	>60
5x	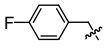	<0.01	0.12	0.14	>1	>60
5y		0.03	0.091	0.046	>33	>60[e]

[a] See Ref. 7.
[b] See Refs. 5 (for assay methods and experimental errors) and 8.
[c] See Refs. 6 (for assay method and experimental error) and 9.
[d] Racemic.
[e] Compounds were screened at 1 μM and other compounds were screened at 5 μM.
[f] ND, not determined.

Table 4. In vitro and in vivo (monkeys) DMPK parameters for compounds **3a** and **5a**

Compound[a]	Sol[b] (μM)	P_{app}[c] (cm/s) $\times 10^{-6}$ (AB)	MLM[d] $t_{1/2}$ (min)	P_{app} BA/AB ratio	*n*	CL (iv) (mL/min/kg)	V_{ss} (iv) (L/kg)	AUC_{inf} (ng/h/mL)	C_{12h}(po)/EC_{50}	F_{po}[e] (%)
3a	55	0.016	>60	2375	2 (po) 2 (iv)	9.0	0.096	124 (po) 10,543 (iv)	0.96	1[f]
5a	44	0.060	22	214	8 (po) 6 (iv)	5.0	0.039	241 (po) 17,640 (iv)	0.66	1

[a] Dose: 5 mg/kg in cynomolgus monkeys.
[b] Solubility in H_2O at pH 7.4.
[c] The Caco-2 assay conditions are described in Ref. 15. Controls: P_{app} Atenolol (low) = 0.40×10^{-6} cm/s, P_{app} Propranolol (high) = 10×10^{-6} cm/s.
[d] The monkey liver microsomal (MLM) assay conditions are described in Ref. 16. MLM data were collected with 5 μM of compounds.
[e] Formulation (both iv and po administrations): 1% DMSO, 9.9% Cremophor EL in 50 mM sodium phosphate buffer, pH 7.4 (compound **3a**) or 5% *N*,*N*-dimethylacetamide, 9.5% Cremophor EL in 50 mM sodium phosphate buffer, pH 7.4 (compound **5a**).
[f] F_{po} = 2% with 1 mg/kg dose of compound **3a** in cynomolgus monkeys; *n* = 8 (po), 8 (iv).

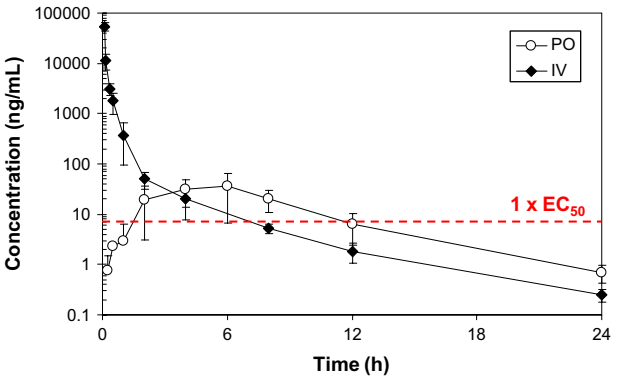

Figure 3. Plasma concentrations of compound **5a** at different times (h) after a single dose of 5 mg/kg in cynomolgus monkeys (administered both iv and po).

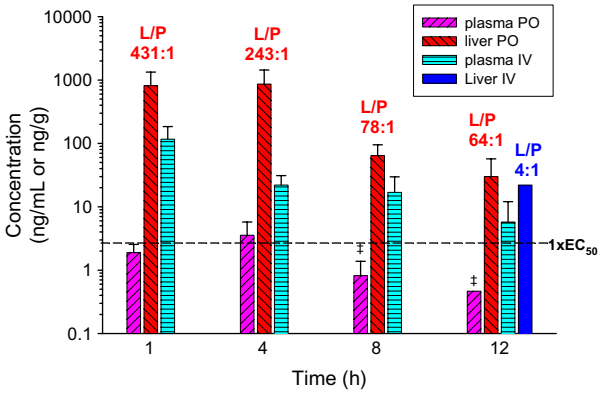

Figure 4. The plasma and liver concentrations and the ratios of the liver to plasma concentrations of **3a** at different times (h) after a single administration (iv and po) to Sprague–Dawley rats with 3 mg/kg dose. The liver concentrations at 1, 4, and 8 h after iv administration were not determined. The dashed line shows the antiviral 1b EC_{50} value in ng/mL for compound **3a**.

area (PSA) = 203 Å^2 for both compounds) which places them considerably outside the polarity range typically associated with gut-permeable molecules (PSA < 140 Å^2).[17] In addition, P_{app} BA/AB ratios for both compounds **3a** and **5a** were very high suggesting that the low oral bioavailabilities may be partially due to their ability to serve as efficient efflux substrates. In spite of the low oral bioavailabilities exhibited by **3a** and **5a**, we found that the plasma concentrations of both compounds 12 h after oral administration to monkeys were close to their corresponding antiviral EC_{50} values (Table 4 and Fig. 3).

As the liver is a major site of HCV replication, we also conducted a PK study with **3a** in Sprague–Dawley rats in order to measure the liver concentrations of the compound.[18] As shown in Figure 4, this study revealed that the concentration of **3a** in rat liver after oral administration was considerably higher than that in plasma for all time points examined. The oral liver/plasma (L/P) ratios declined over time, but consistent with the liver being the organ initially exposed to orally dosed agents, remained higher than the corresponding L/P ratios observed 12 h after iv administration of **3a**. Importantly, the concentration of **3a** in rat liver 12 h after po administration substantially exceeded its antiviral EC_{50} value (C_{12h}/EC_{50} = 24).[19] The high L/P ratio (64:1 12 h post oral dose) implied the tendency of **3a** to accumulate at a major site of HCV replication and this property may enhance its ability to function as an effective anti-HCV agent in vivo.

For the synthesis of the pyridazinone derivatives bearing sulfonamide R^3 moieties (**1a**, **10**, and **11**), three routes (A, B, and C) were used most often as shown in Scheme 1. In Route A, ester **6**[20] was condensed with 2-aminobenzensulfonamide **7a**[21] by heating in pyridine to generate the corresponding amide intermediates, which were then cyclized in the presence of DBU in pyridine to yield the desired compound **1a**. In Route B, hydrazone **8**[20] was coupled with acids **9a**[22] in the presence of DCC or EDC to form the corresponding amide intermediates which were further cyclized in the presence of NaOEt in absolute ethanol to form the desired compound **1a**. In Route C, compound **1b** bearing an iodo group at the 7-position was transformed to the corresponding sulfonamide analogs **10** or **11** via CuI catalyzed displacement of the iodo atom.[23] Compound **1b** (R^3 = I) was prepared using Route A (from compounds **6** and **7b**[22]) or Route B (from compounds **8** and **9b**[22]). Alternatively, the *N*-alkylated sulfonamide analog **11** was also accessed via alkylation of the unsubstituted sulfonamide **10**.

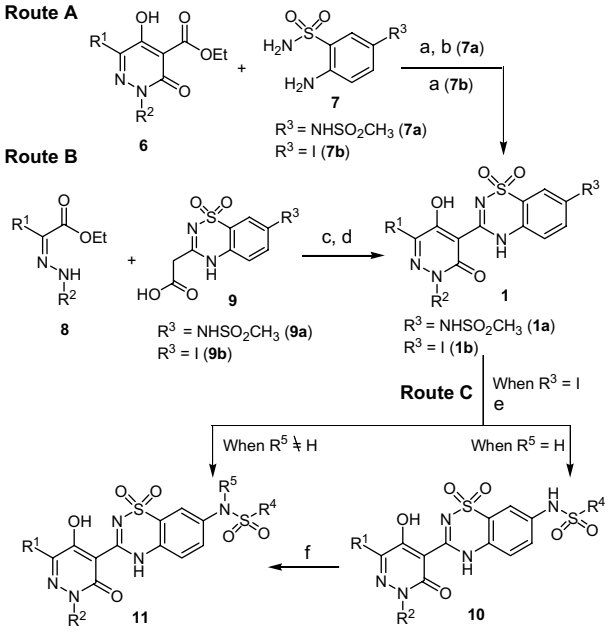

Scheme 1. Reagents and conditions: (a) pyridine, 120 °C, 3 h; (b) pyridine, DBU (2–4 equiv), 120 °C, 16 h, 12–43% over two steps; (c) DCC, CH_2Cl_2/DMF, or EDC, NMM, DMF, rt, 12 h; (d) NaOEt, EtOH, rt or 50–60 °C, 8–12 h, 13–50% over two steps; (e) $NHR^5SO_2R^4$, CuI, sarcosine, K_3PO_4, DMF, 100 °C, 4–16 h, 12–52%; (f) R^5-X (X = Cl, I), NaH, DMF, rt, 35–92%.

In summary, we synthesized a number of highly potent inhibitors of genotype 1 HCV NS5B polymerase, with single digit nM antiviral potency, derived from pyridazinones with a methylsulfonamide R^3 substituent. Our SAR studies revealed that R^1 and R^3 substituents significantly affected the HLM stability of the resulting molecules. A PK study in monkeys with the highly potent inhibitor **5a** (1b EC_{50} = 16 nM) using a single 5 mg/kg oral dose showed poor oral bioavailability, but C_{12h} in plasma was close to its EC_{50} value. In addition, the ratio of liver to plasma concentrations in rat of another very potent inhibitor **3a** (1b EC_{50} = 5 nM) 12 h after a single oral dose of 3 mg/kg was very high (64-fold), and this property may be beneficial since liver is a major site of HCV replication. The further optimization of the PK properties of this series of inhibitors will be discussed in a future communication.

Acknowledgments

The authors thank Drs. Devron Averett and Steve Worland for their support and helpful discussions during the course of this work.

References and notes

1. (a) Kim, W. R. *Hepatology* **2002**, *36*, 30; (b) Alter, M. J.; Kruszon-Moran, D.; Nainan, O. V.; McQuillan, G. M.; Gao, F.; Moyer, L. A.; Kaslow, R. A.; Margolis, H. S. *N. Eng. J. Med.* **1999**, *341*, 556; (c) Alberti, A.; Benvegnu, L. *J. Hepatol.* **2003**, *38*, S104.
2. (a) Sidwell, R. W.; Huffman, J. H.; Khare, G. P.; Allen, L. B.; Witkowski, J. T.; Robins, R. K. *Science* **1972**, *177*, 705; (b) Smith, R. A.; Kirkpatrick, W.. In *Ribavirin, a Broad Spectrum Antiviral Agent*; Academic Press: New York, 1980; vol. xiii, pp. 237; (c) De Clercq, E. *Adv. Virus Res.* **1993**, *42*, 1.
3. Hoofnagle, J. H.; Seeff, L. B. *N. Eng. J. Med.* **2007**, *355*, 2444.
4. (a) Kolykhalov, A. A.; Agapov, E. V.; Blight, K. J.; Mihalik, K.; Feinstone, S. M.; Rice, C. M. *Science* **1997**, *277*, 570; (b) Koch, U.; Narjes, F. *Curr. Top. Med. Chem.* **2007**, *7*, 1302.
5. Zhou, Y.; Webber, S. E.; Murphy, D. E.; Li, L.-S.; Dragovich, P. S.; Tran, C. V.; Sun, Z.; Ruebsam, F.; Shah, A. M.; Tsan, M.; Showalter, R. E.; Patel, R.; Li, B.; Zhao, Q.; Han, Q.; Hermann, T.; Kissinger, C. R.; LeBrun, L.; Sergeeva, M. V.; Kirkovsky, L. *Bioorg. Med. Chem. Lett.* **2008**, *18*, 1413.
6. Zhou, Y.; Li, L.-S.; Dragovich, P. S.; Murphy, D. E.; Tran, C. V.; Ruebsam, F.; Webber, S. E.; Shah, A. M.; Tsan, M.; Averill, A.; Showalter, R. E.; Patel, R.; Han, Q.; Zhao, Q.; Hermann, T.; Kissinger, C. R.; LeBrun, L.; Sergeeva, M. V. *Bioorg. Med. Chem. Lett.* **2008**, *18*, 1419.
7. All structures of compounds under study were consistent with ^{1}H NMR and LC–MS analysis ($\geqslant$95% HPLC purity). They are arbitrarily drawn in one of the possible tautomer forms.
8. Potencies of compounds with IC_{50} values below 10 nM cannot be distinguished from each other using the 1b biochemical assay because this is the lower limit imposed by the enzyme concentration. The EC_{50} values for these compounds, however, do provide a comparative measure of potency.
9. Potencies of compounds with IC_{50} values below 25 nM cannot be distinguished from each other using the 1a biochemical assay because this is the lower limit imposed by the enzyme concentration.
10. Other thiadiazine or thiazine-containing NS5B inhibitors bearing sulfonamide R^3 fragments have been reported: (a) Krueger, A. C.; Madigan, D. L.; Green, B. E.; Hutchinson, D. K.; Jiang, W. W.; Kati, W. M.; Liu, Y.; Maring, C. J.; Masse, S. V.; McDaniel, K. F.; Middleton, T. R.; Mo, H.; Molla, A.; Montgomery, D. A.; Ng, T. I.; Kempf, D. J. *Bioorg. Med. Chem. Lett.* **2007**, *17*, 2289; (b) Blake, F. J. et al. U.S. Patent US20060040972, 2006.
11. Crystals of HCV NS5B polymerase (genotype 1b, strain BK, Δ21) were grown by the hanging drop method at room temperature using a well buffer of 20% PEG 4K, 50 mM ammonium sulfate, 100 mM sodium acetate, pH 4.7 with 5 mM DTT. The crystals formed in space group P212121 with approximate cell dimensions, a = 85 Å, b = 106 Å, c = 127 Å containing two protein molecules in the asymmetric unit. Protein–inhibitor complexes were prepared by soaking these NS5B crystals for 3–24 h in solutions containing 15–20% DMSO, 20% glycerol, 20% PEG 4K, 0.1 M Hepes, 10 mM $MgCl_2$ at pH 7.6 and inhibitors at concentrations of 2–10 mM. Diffraction data were collected to a resolution of 2.1 Å for compound **3a**. This crystal structure has been deposited in the Protein Databank (www.rcsb.org) with entry code: 3CDE. Full details of structure determination are given in the respective PDB entries.
12. The reduced flexibility of the R^3 –$NHSO_2CH_3$ fragment relative to the –$OCH_2C(O)NH_2$ moiety may also contribute to the improved potency of **3a**.
13. The inability of the –SO_2– moieties present in compounds **3i–q** to duplicate the favorable H-bonding interactions observed in the **3a**–NS5B co-crystal structure may also

contribute to the weaker biological potencies observed for these molecules.
14. Genotype 1b NS5B IC_{50} values below 10 nM cannot be accurately compared to the corresponding EC_{50} values due to the limitation of the biochemical assay.
15. Assay condition for Caco-2: Express three day Caco-2 cell cultures (Celsis/IVT, Baltimore, MD) were used on 24-well polycarbonate membrane inserts. The integrity of the monolayers was confirmed by measurement of the trans-epithelial electrical resistance (TEER) and the apparent permeability of the fluorescent marker compound lucifer yellow. Apparent permeabilities of a series of test articles and of selected control compounds were determined in duplicate at a single concentration of 10 μM in the apical to basolateral direction at 37 °C. The basolateral compartments were sampled for up to 3 h after compound addition to the apical compartment (collecting a total of four times points) and were analyzed for test article content by LC/MS/MS. Samples from the final apical compartments were also collected and analyzed. The apparent permeability of each test article was calculated from these data.
16. Monkey liver microsomal half-life (MLM $t_{1/2}$) assay conditions: The final concentrations in the assay were 0.5 mg/mL monkey liver microsomes, 5 μM test article, 3.3 mM glucose-6-phosphate, 1.3 mM $NADP^+$, and 0.4 U/mL glucose-6-phosphate dehydrogenase in 50 mM potassium phosphate (pH 7.4) and 3.3 mM $MgCl_2$ buffer. Samples were incubated at 37 °C. At 0, 5, 10, 20, 30, 45, and 60 min, the reactions were terminated by removing 125 μL-aliquots and quenching in 375 μL of ACN. The samples were vortexed and centrifuged. The supernatant was removed and dried under nitrogen. The dried samples were reconstituted in 2% DMSO in water and analyzed by LC/MS/MS for the remaining parent molecules. The $t_{1/2}$ values were determined by fitting the data to a single exponential decay curve. Comparison of $t_{1/2}$ values from multiple replicate experiments on a representative compound gave a 16% standard deviation from the mean value.
17. (a) Palm, K.; Stenberg, P.; Luthman, K.; Artursson, P. *Pharm. Res.* **1997**, *14*, 568; Our PSA values were calculated by a different method according to the method as described in (b) Ertl, P.; Rohde, B.; Selzer, P. *J. Med. Chem.* **2000**, *43*, 3714.
18. The PK parameters of compound **3a** in rats: $n = 12$ (po) and 3 (iv); CL (iv) = 13.8 (mL/min/kg); V_{ss} (iv) = 0.453 (L/kg); $AUC_{inf} = 27$ (po); 3631 (iv) (ng/h/mL); C_{12h}(po)/$EC_{50} = 0.35$; $F_{po} = 1\%$.
19. The ratio of the C_{12h}(liver)/EC_{50} was calculated assuming the density of the liver was 1.
20. The procedures for the synthesis of compounds **6** and **8** are described in (a) Li, L.-S.; Zhou, Y.; Zhao, J.; Dragovich, P. S.; Stankovic, N.; Bertolini, T. M.; Murphy, D. E.; Sun, Z.; Tran, C. V.; Ayida, B. K.; Ruebsam, F.; Webber, S. E. *Synthesis* **2007**, 3301; (b) Murphy, D. E.; Dragovich, P. S.; Ayida, B. K.; Bertolini, T. M.; Li, L.-S.; Ruebsam, F.; Stankovic, N. S.; Sun, Z.; Zhao, J.; Zhou, Y. *Tetrahedron Lett.* **2008**, *49*, 811.
21. Intermediate **7a** was prepared using modified literature procedures as described in (a) Krueger, A. C.; Madigan, D. L.; Green, B. E.; Hutchinson, D. K.; Jiang, W. W.; Kati, W. M.; Liu, Y.; Maring, C. J.; Masse, S. V.; McDaniel, K. F.; Middleton, T. R.; Mo, H.; Molla, A.; Montgomery, D. A.; Ng, T. I.; Kempf, D. *J. Bioorg. Med. Chem. Lett.* **2007**, *17*, 2289; (b) Hutchinson, D. K. et al. U.S. Patent 2005/0107364; (c) Goldfarb, A. R.; Berk, B. *J. Am. Chem. Soc.* **1943**, *65*, 738; (d) Dragovich, P. S.; Murphy, D. E.; Tran, C. V.; Ruebsam, F. *Synth. Commun.*, **2008**, in press.
22. The procedures for the synthesis of **7b** and **9a**–**b** are described in Ruebsam, F.; Tran, M. T.; Webber, S. E.; Dragovich, P. S.; Li, L.-S.; Murphy, D. E.; Kucera, D. J.; Sun, Z.; Tran, C. V. PCT International Patent Application WO 2007150001 A1, 2007. The synthesis of **3m** containing a cyclic sulfone R^3 moiety was similar to that described in the above patent. The syntheses of compounds **3l**–**q** will be discussed elsewhere.
23. Deng, W.; Liu, L.; Zhang, C.; Liu, M.; Guo, Q.-X. *Tetrahedron Lett.* **2005**, *46*, 7295.